International Journal of Cardiology 388 (2023) 131162

Contents lists available at ScienceDirect

International Journal of Cardiology

journal homepage: www.elsevier.com/locate/ijcard

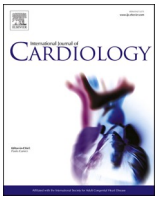

Left ventricular deformation and myocardial fibrosis in pediatric patients with Duchenne muscular dystrophy

Thijs P. Kerstens [a,1], Wouter M. van Everdingen [b,1], Jesse Habets [c,1], Arie P.J. van Dijk [d,1], Willem A. Helbing [e,1], Dick H.J. Thijssen [a,f,1], Floris E.A. Udink ten Cate [g,1,*]

[a] Department of Medical BioSciences, Radboud University Medical Center, Geert Grooteplein Zuid 10, Nijmegen 6525 GA, the Netherlands
[b] Department of Radiology, Nuclear Medicine, and Anatomy, Radboud University Medical Center, Geert Grooteplein Zuid 10, Nijmegen 6525 GA, the Netherlands
[c] Department of Radiology and Nuclear Medicine, Haaglanden Medical Center, Lijnbaan 32, The Hague 2512 VA, the Netherlands
[d] Department of Cardiology, Radboud University Medical Center, Geert Grooteplein Zuid 10, Nijmegen 6525 GA, the Netherlands
[e] Department of Pediatrics, Division of Cardiology, Erasmus MC-Sophia Children's Hospital, Dr Molewaterplein 40, Rotterdam 3015 GD, the Netherlands
[f] Research Institute for Sport and Exercise Sciences, Liverpool John Moores University, Liverpool L3 5UX, United Kingdom
[g] Academic Center for Congenital Heart Disease (ACAHA), Department of Pediatric Cardiology, Amalia Children's Hospital, Radboud University Medical Center, Nijmegen, the Netherlands

ARTICLE INFO

Keywords:
Duchenne muscular dystrophy
Cardiomyopathy
LV deformation
Strain
Rotation
Fibrosis

ABSTRACT

Background: Left ventricular (LV) strain and rotation are emerging functional markers for early detection of LV dysfunction and have been associated with the burden of myocardial fibrosis in several disease states. This study examined the association between LV deformation (i.e., LV strain and rotation) and extent and location of LV myocardial fibrosis in pediatric patients with Duchenne muscular dystrophy (DMD).

Methods and results: 34 pediatric patients with DMD underwent cardiovascular magnetic resonance (CMR) with late gadolinium enhancement (LGE) to assess LV myocardial fibrosis. Offline CMR feature-tracking analysis was used to assess global and segmental longitudinal and circumferential LV strain, and LV rotation. Patients with fibrosis (n = 18, 52.9%) were older than those without fibrosis (14 ± 3 years (yrs) vs 11 ± 2 yrs., p = 0.01). There was no significant difference in LV ejection fraction (LVEF) between subjects with and without fibrosis (54 ± 6% vs 56 ± 4%, p = 0.18). However, lower endocardial global circumferential strain (GCS), but not LV rotation, was associated with presence of fibrosis (adjusted Odds Ratio 1.25 [95% CI 1.01–1.56], p = 0.04). Both GCS and global longitudinal strain correlated with the extent of fibrosis (r = .52, p = 0.03 and r = .75, p < 0.01, respectively). Importantly, segmental strain did not seem to correspond to location of fibrosis.

Conclusion: A lower global, but not segmental, strain is associated with presence and extent of LV myocardial fibrosis in pediatric DMD patients. Therefore, strain parameters might detect structural myocardial alterations, however currently more research is needed to evaluate its value (e.g., prognostic) in clinical practice.

1. Introduction

Duchenne muscular dystrophy (DMD) is an X-linked recessive dystrophinopathy affecting approximately 1 in 6500 live male births [1,2]. DMD is caused by mutations in the DMD gene (Xp21.2) resulting in a deficiency of functional dystrophin, a vital protein that connects the cytoskeleton of myofibers to the extracellular matrix and membrane proteins [3]. Patients diagnosed with DMD suffer from progressive muscle degeneration and weakness that leads to loss of ambulation around 12 years old, development of cardiac and respiratory complications, and eventually death, typically in the late twenties to early thirties [3–6].

The leading cause of death in DMD is cardiomyopathy. Approximately 90% of DMD patients develop a dilated cardiomyopathy by the age of 18 [3,7]. The progressive degeneration of cardiomyocytes leads to the appearance of fibrosis, typically in the epicardial posterobasal segments of the left ventricle (LV) [3,8]. Therefore, DMD patients need periodic imaging to evaluate cardiac function and start timely treatment to delay the onset of fibrosis, as this process contributes to development of heart failure [9]. Currently, common clinical practice for monitoring

* Corresponding author at: Department of Pediatric Cardiology (840), Radboud University Medical Center, P.O. Box 9101, Nijmegen 6500 HB, the Netherlands.
E-mail address: floris.udinktencate@radboudumc.nl (F.E.A. Udink ten Cate).
[1] This author takes responsibility for all aspects of the reliability and freedom from bias of the data presented and their discussed interpretation

https://doi.org/10.1016/j.ijcard.2023.131162
Received 26 May 2023; Received in revised form 30 June 2023; Accepted 5 July 2023
Available online 9 July 2023

cardiac function predominantly relies on changes in LV ejection fraction (LVEF). However, LVEF lacks sensitivity to detect subtle signs of myocardial dysfunction [10,11]. For example, global strain parameters have previously detected cardiac dysfunction in DMD patients with preserved LVEF using CMR tagging [12]. Given the occurrence of fibrosis predominantly in specific regions, also segmental strain might be altered, although it is unclear whether this can detect fibrosis [11,13–15]. Additionally, changes in LV rotation seem present in dilated cardiomyopathy [16–18], possibly before any changes in LVEF [19]. Combining CMR-feature tracking (FT) for strain and rotation analysis and quantitative evaluation of fibrosis could present additional functional markers to aid in detection and monitoring cardiac function and treatment evaluation without the need for additional CMR sequences.

Therefore, the aim of this research was to explore the association of LV strain measures (i.e., global and segmental, longitudinal and circumferential) and LV rotational mechanics (e.g., twist and torsion) assessed with CMR-FT and the presence and extent of myocardial fibrosis. Our hypothesis was that decreased strain and rotation would be associated with the presence and the extent of LV myocardial fibrosis. Furthermore, we explored the relationship between segmental strain parameters and location of fibrosis.

2. Methods

2.1. Study design and population

This study included DMD patients who underwent clinically indicated CMR imaging with LGE between June 2017 and November 2021 at the Radboud University Medical Center in Nijmegen, The Netherlands. Patients were excluded from the analysis if they did not consent to share their personal medical data or if they had other cardiovascular pathologies than DMD. Cine CMR images were excluded from the feature-tracking analysis in case of inadequate image quality due to artifacts. Patient characteristics such as age, weight, height, systolic and diastolic blood pressure, were obtained from medical records within six months of the CMR. The study was approved by the local institutional review board. This retrospective research was performed according to the local code of research conduct and data protection rules. Clinical research data was stored using the online Castor Electronic Data Capture (Ciwit B.V., Amsterdam, The Netherlands).

2.2. CMR acquisition & volumetric data

CMR imaging was performed as part of routine clinical care on a Siemens Avanto 1.5 T scanner system (Siemens, Erlangen, Germany) according to a standardized protocol by experienced CMR technicians and without administering any sedatives. Images were acquired with electrocardiogram triggering and during breath-hold. A multiphase and multislice volumetric data set was acquired covering ventricles from base to apex in short-axis orientation using fast 2-dimensional steady-state free precession (SSFP) scan. The following MRI acquisition parameters were used: repetition time (TR) 44.25 ms, echo time 1.25 ms, flip angle 78°, and slice thickness 5.0 mm with 1.0 mm interslice gap. Heart rate limited the number of reconstructed phases, a minimum of 25 phases for SSFP was used.

Standard two-, three-, and four-chamber SSFP cine images were obtained. Parameters used to assess biventricular dimensions and function were end diastolic volume (EDV), end systolic volume (ESV), ejection fraction (EF), and stroke volume (SV) of both ventricles. Furthermore, interventricular septal thickness (IVSd) and posterior wall thickness (PWd) were measured at end diastole on basal short axis images. Volumetric data were indexed to body surface area (BSA).

An intravenous dose of 0.3 mL/kg of the gadolinium-based contrast agent 'Dotarem' (Guerbet, France) was administered to the patient. At least 10 minutes after administration LGE series were acquired. LGE series included left ventricular two-, three-, and four-chamber planes and short-axis LGE stacks covering the left ventricle excluding the apical cap. A cardiovascular radiologist (W.E.) assessed LGE location and severity, inconclusive findings were discussed until consensus was reached with an experienced cardiovascular radiologist (J.H.). The extent of fibrosis was quantified as percentage of LV myocardium affected (LV scar %) using Segment version 3.1, R8109 (http://segment.heiberg.se) [20].

2.3. LV strain measurements

Offline CMR-FT analysis was performed using QStrain (Medis Medical Imaging, Leiden, The Netherlands) to quantify global and segmental end-systolic peak circumferential and longitudinal LV strain. A 17-segment software-generated model was acquired for longitudinal strain, while a 16-segment model was obtained for circumferential strain since the apical cap, i.e. segment 17, is not visible on the short-axis images [21]. On every image, the epi- and endocardial borders were manually traced in both end-systole and end-diastole. Subsequently, an automatic computation was triggered, by which the software algorithm tracked the outlined border throughout the cardiac cycle. All CMR analyses were performed by one researcher (T.K.) under the supervision of a radiologist (W.E.). Endocardial longitudinal strain was derived from apical four-, three- and two-chamber views. Endocardial and myocardial circumferential strain was derived from apical, mid-ventricular (i.e., level of papillary muscles) and basal short-axis slices. Following visual inspection of tracking quality by W.E. and T.K., segments with unreliable tracing were excluded from the strain analysis, with a maximum of two segments per view. In line with recommendations, all references to strain changes consider absolute values, i.e., an increase means a more negative value [22].

2.4. LV rotation analysis

Rotational parameters (e.g., twist and torsion) were derived from apical and basal short-axis slices. The end-systolic marker was based on minimal LV volume on long-axis images or minimal LV diameter on short-axis images. Results were exported from QStrain and processed in Microsoft Excel (version 2102, Microsoft Corp., Redmond, WA, USA) to acquire twist, torsion, twist rate, and diastolic untwist rate. In this study, LV twist (°) was defined as the systolic peak difference between rotations (φ) of the apex (counter clockwise, positive values) and the base (clockwise, negative values), as viewed from the apex [23].

$$LV\ Twist = \varphi_{apex} - \varphi_{base} \tag{1}$$

LV torsion (°/cm), defined as normalized twist, was calculated as LV twist divided by the distance (D) between the short-axis planes at the base and apex used for the feature-tracking analysis, as measured on the four-chamber apical view (Apical – basal slice distance).

$$LV\ Torsion = \frac{\left(\varphi_{apex} - \varphi_{base}\right)}{D} \tag{2}$$

2.5. Statistical analysis

Statistical analysis was performed using R version 4.0.4 [24]. All parameters were inspected for normality using histograms, Q-Q plots, and the Shapiro-Wilk test. Continuous variables were reported as mean ± standard deviation (SD) or median [interquartile range] and categorical variables as number and proportions (n (%)). Differences between groups were assessed using a *t*-test or a non-parametric equivalent. Proportions were tested using chi-squared tests or Fisher's exact tests. First, to assess the association between CMR parameters and the presence of fibrosis, logistic regression was used. Variables were selected based on univariable logistic regression ($P < 0.1$) and adjusted for age in a multivariable logistic regression model. The assumption of linearity between the continuous predictors and the logit transformation

of the outcome variable was tested using Box-Tidwell tests. Multicollinearity was checked using variance inflation factors. Second, to explore the correlation between strain parameters and the extent of fibrosis (LV scar %), Pearson bivariate correlation analysis was used. Cases with 0% LV scar were excluded from this analysis. Third, to compare the segmental strain pattern with fibrosis location, LV bullseye plots were constructed using the mean segmental values for both patients with and without fibrosis. The difference per segment (no fibrosis - fibrosis) was calculated and compared with the pattern of distribution of fibrosis. Bullseye plots were constructed using Google Colaboratory (Python 3.6.9, Google LLC, Mountain View, CA, USA). *P*-values of <0.05 were considered significant.

3. Results

A total of 35 DMD patients were eligible for this cohort. However, one patient (2%) was excluded from the analysis due to low quality CMR. Resulting in a total of 34 patients included in the final analysis, of which 18 had fibrosis and 16 had no fibrosis based on LGE. Mean age at the time of CMR was 14.1 ± 2.7 and 11.9 ± 2.0 years old ($p < 0.01$) in the group with fibrosis and without fibrosis, respectively. *Z*-scores for height and weight were not significantly different between groups. At the time of CMR the average duration of glucocorticoid treatment was 7.8 ± 3.9 and 5.1 ± 2.7 years ($p = 0.03$) in the fibrosis and no fibrosis groups, respectively. We found no between-group differences in other anthropometric measurements, hemodynamic parameters, and frequency of ACE-inhibitor use before CMR (Table 1). Moreover, no difference between LVEF was found between groups (fibrosis: 56 ± 4%, no fibrosis: 54 ± 6%, $p = 0.18$) (Table 1).

3.1. Presence of fibrosis

A significant between-group difference was found for endocardial global circumferential strain (GCS) (fibrosis: −27.8 ± 5.0 vs. no fibrosis: −31.4.0 ± 4.3) and myocardial GCS (fibrosis: −18.9 ± 4.2 vs. no fibrosis: −22.0 ± 3.1) (Table 2). In univariable analysis both endocardial and myocardial GCS were associated with presence of fibrosis (Table 3). After adjusting for age, endocardial GCS remained significantly associated with fibrosis (Adjusted Odds Ratio (OR) 1.25, 95% CI [1.01–1.56], $p = 0.043$) per unit decrease in endocardial GCS. Endocardial GCS ranged from −38.6 to −18.5 in this cohort. The distance measured between the basal and apical short axis slice, used to calculate torsion, did differ (fibrosis: 38 ± 5 mm vs. no fibrosis: 34 ± 6 mm, $p = 0.05$). None of the rotational parameters, i.e., twist, torsion, twist rate, or diastolic untwist rate were found to be associated with the presence of fibrosis (Table 3).

Table 1
Cohort characteristics of the study population at the time of CMR.

	No Fibrosis (*N* = 16)	Fibrosis (*N* = 18)	*P-value*
Age, years	11.9 ± 1.98	14.1 ± 2.69	0.009
Weight, kg	45 [39–58]	62 [50–82]	0.067
Weight, z-score	0.733 ± 1.29	1.01 ± 1.27	0.530
Height, cm	143 ± 15	158 ± 16	0.008
Height, z-score	−0.874 ± 1.39	−0.406 ± 1.43	0.340
BMI, z score	1.27 ± 1.02	1.17 ± 1.32	0.810
Heart rate, bpm	101 ± 17.5	95.3 ± 15.2	0.357
SBP, mmHg	106 ± 14.2	109 ± 11.3	0.468
Missing, n (%)	0 (0%)	1 (5.6%)	
DBP, mmHg	63.4 ± 9.7	63.1 ± 7.3	0.916
Missing, n (%)	0 (0%)	1 (5.6%)	
Duration glucocorticoids treatment, years	5.1 ± 2.7	7.8 ± 3.9	0.027
Missing, n (%)	0 (0%)	1 (5.6%)	
ACE-inhibitor, n (%)	3 (18.8%)	3 (16.7%)	1.000

Data are reported as n(%) for categorical variables and mean ± SD. Age at time of CMR. BMI, body mass index; SBP, systolic blood pressure; DBP, diastolic blood pressure; ACE, angiotensin-converting-enzyme.

Table 2
Conventional CMR parameters and LV deformation parameters for both groups.

	No Fibrosis (N = 16)	Fibrosis (N = 18)	*P-value*
Conventional Measures			
LVEDV indexed, ml/m^2	64.4 ± 10.1	68.9 ± 12.2	0.253
LVESV indexed, ml/m^2	28.3 ± 6.1	31.7 ± 6.9	0.144
LVEF, %	56.4 ± 3.8	54.0 ± 6.3	0.181
IVSd. mm	5.8 ± 1.0	6.2 ± 1.5	0.290
PWd, mm	5.0 [5.0–5.3]	6.0 [5.0–6.0]	0.070
Apical – basal slice distance, mm	33.6 ± 5.9	37.8 ± 5.5	0.043
RVEDV indexed, ml/m^2	58.5 ± 10.0	58.4 ± 10.3	0.969
RSESV indexed, ml/m^2	24.3 ± 6.6	24.7 ± 5.3	0.822
RVEF, %	58.9 ± 6.4	57.3 ± 7.2	0.499
LV Deformation			
Endo GLS, (%)	−23.1 ± 2.77	−22.5 ± 3.32	0.517
Myo GCS, (%)	−22.0 ± 3.09	−18.9 ± 4.21	0.017
Endo GCS, (%)	−31.4 ± 4.29	−27.8 ± 5.04	0.031
Endo twist, (°)	10.0 ± 12.6	5.83 ± 9.19	0.284
Myo twist, (°)	9.39 ± 7.42	6.85 ± 5.65	0.277
Myo Torsion, (°/cm)	2.76 ± 2.07	1.82 ± 1.59	0.152
Endo Torsion, (°/cm)	2.67 ± 3.36	1.72 ± 2.54	0.365
Myo twist rate, (°/s)	97.4 [85.4–147]	95.8 [68.4–118]	0.191
Missing, n (%)	0 (0%)	1 (5.6%)	
Myo diastolic untwist rate, (°/s)	−88.8 [−152 - −73.4]	−86.4 [−103 - −64.7]	0.445
Missing, n (%)	0 (0%)	2 (11.1%)	
Endo twist rate, (°/s)	157 [42.6–196]	120 [−44.6 – 147]	0.144
Missing, n (%)	0 (0%)	1 (5.6%)	
Endo diastolic untwist rate, (°/s)	−172 [−265 - −46.9]	−122 [−144 – 33.4]	0.075
Missing, n (%)	0 (0%)	2 (11.1%)	
Rigid body rotation, n (%)	5 (31.3%)	7 (38.9%)	0.729

Data are reported as n(%) for categorical variables and mean ± SD or median [interquartile range] for continuous variables. Indexed volumes are represented. LVEDV, left ventricular end diastolic volume; LVESV, left ventricular end systolic volume; LVEF, left ventricular ejection fraction; IVSd, interventricular septum thickness in diastole; PWd, posterior wall thickness in diastole; RVEDV, right ventricular end diastolic volume; RVESV, right ventricular end systolic volume; RVEF, right ventricular ejection fraction. Endo = endocardial; Myo = myocardial; GLS = Global longitudinal strain; GCS = Global circumferential strain; TSR = Torsion-to-shortening ratio. Variables are mean ± SD, median [interquartile range] or n (%).

3.2. Extent of fibrosis

In patients with fibrosis, mean extent of fibrosis (LV scar %) was 11.2 ± 7.2%. The correlation between LVEF, strain, and rotational parameters and LV scar % is presented in Table 4. LVEF was negatively correlated with the extent of LV fibrosis ($r(16) = -.61$, $p < 0.01$; Fig. 1A). Endocardial GCS ($r(16) = .52$, $p = 0.03$), myocardial GCS ($r(16) = .65$, $p < 0.01$), and endocardial GLS ($r(16) = .75$, $p < 0.01$) were positively correlated with LV scar % (Fig. 1B-D). Rotational parameters were not correlated with the extent of fibrosis.

3.3. Segmental strain and location of fibrosis

Delayed enhancement was mainly present in the anterolateral and inferolateral wall of the left ventricle, i.e., in segments 5, 6, 11, and 12 in 89%, 56%, 83%, and 44% of the cases with fibrosis ($n = 18$), respectively. The apical septal segment was not affected by fibrosis in the cases observed (Fig. 2). As shown in Fig. 2, the segments with largest segmental strain difference between groups did not correspond to the segments with a higher prevalence of fibrosis.

Table 3
Odds ratios and 95% confidence intervals for the logistic regression of the association between deformation and presence of fibrosis.

	Univariable Analysis		Multivariable Analysis	
	OR (95% CI)	*P-value*	*OR (95% CI)*	*P-value*
LVEF (%)	0.91 (0.78–1.05)	0.198		
Endo GLS (%)	1.08 (0.86–1.36)	0.511		
Myo GCS (%)	1.27 (1.02–1.57)	0.030	1.29 (0.99–1.68)	0.062
Endo GCS (%)	1.18 (1.01–1.39)	0.042	1.27 (1.01–1.59)	0.043
Myo twist (°)	0.94 (0.84–1.04)	0.267		
Endo twist (°)	0.96 (0.90–1.03)	0.274		
Myo Torsion (°/cm)	0.74 (0.49–1.12)	0.152		
Endo Torsion (°/cm)	0.89 (0.70–1.14)	0.350		
Endo twist rate (°/s)	1.00 (0.99–1.00)	0.234		
Myo twist rate (°/s)	0.99 (0.98–1.00)	0.131		
Endo diastolic untwist rate (°/s)	1.00 (1.00–1.01)	0.101		
Myo diastolic untwist rate (°/s)	1.00 (0.99–1.01)	0.420		
Rigid body rotation (ref: no)	1.40 (0.34–5.79)	0.642		

Odds ratio per unit increase (i.e., towards 0 for negative values), except for categorical variables which is relative to the reference category. Odds ratios were adjusted for age when $p < 0.1$.
LVEF = Left ventricular ejection fraction; Endo = endocardial; Myo = myocardial; GLS = Global longitudinal strain; GCS = Global circumferential strain; ref = reference category.

Table 4
Pearson correlation coefficients for the relation between deformation parameters and LV scar %.

	Pearson's Correlation (r)	*P-value*
LVEF (%)	−.607	0.007
Endo GLS (%)	.752	< 0.001
Myo GCS (%)	.650	0.003
Endo GCS (%)	.520	0.027
Myo twist (°)	−.229	0.360
Endo twist (°)	−.225	0.370
Myo Torsion (°/cm)	−.256	0.305
Endo Torsion (°/cm)	−.281	0.259
Myo twist rate (°/s)	−.229	0.356
Myo diastolic untwist rate (°/s)	.308	0.246
Endo twist rate (°/s)	−.203	0.420
Endo diastolic untwist rate (°/s)	.096	0.704

LVEF = Left ventricular ejection fraction; Endo = endocardial; Myo = myocardial; GLS = Global longitudinal strain; GCS = Global circumferential strain; TSR = Torsion-to-shortening ratio.

4. Discussion

This study presents the following results. First, after adjusting for age, we found that endocardial global circumferential strain was significantly associated with the presence of fibrosis, whilst no association was found for rotational parameters and LVEF. Secondly, we observed that the extent of fibrosis correlated with global circumferential and longitudinal strain parameters, but also with LVEF. Finally, bullseye plots suggested no apparent relation between segmental strain and the location of fibrosis. Taken together, this suggests that global strain parameters may provide relevant information regarding both presence and extent of fibrosis in patients with DMD, possibly even in an early stage of disease.

The association of a lower GCS with presence and extent of LV fibrosis in DMD patients is in line with previous research [25]. This is especially of interest since GCS is suggested to be the most robust and consistent parameter in CMR-FT [26]. Moreover, we found that global longitudinal strain (GLS), an accepted marker for myocardial dysfunction [27], was associated with the extent of but not with the presence of fibrosis. This is in contrast with work by *Raucci* et al., albeit in slightly older patients, more frequently affected with fibrosis, and with worse GCS compared to our cohort [25]. Thus, possibly studying patients in a later stage of cardiac disease. The distinct observations for global longitudinal and circumferential strain suggest that presence and extent of fibrosis affect cardiac mechanics in different ways. Mechanistically, this could be explained by the characteristic subepicardial location of fibrosis in DMD [28]. Subepicardial fibers shorten circumferentially, whereas subendocardial fibers shorten longitudinally [16,29]. Consequently, subepicardial fibrosis might predominantly affect GCS, explaining why this was associated with the presence of fibrosis in our study. Additionally, longitudinal shortening might be attenuated when fibrosis extends towards the sub-endocardium. This may explain the correlation between GLS and the extent of fibrosis. Altogether, suggesting that different strain parameters may be affected at different stages of cardiac disease in DMD. These parameters could provide additional information since recent research suggests that myocardial strain parameters, and possibly a change thereof, seem related to all-cause mortality in this population [30].

In contrast to endocardial GCS, there was no association between myocardial GCS and the presence of fibrosis, although myocardial GCS did correlate with the extent of fibrosis. These differences between endocardial versus myocardial strain may be the result of a higher sensitivity of endocardial (circumferential) strain to detect contractile impairment. Indeed, *Tanacli* et al. observed that endocardial strain was most affected with increasing severity of heart failure and myocardial remodeling [31]. However, the relevance of interlayer differences in strain has been debated [32]. Although myocardial GCS did not significantly relate to the presence of myocardial fibrosis, it is important to consider the relatively small sample size. This is further supported by the corresponding confidence interval of myocardial GCS (Table 3). Therefore, both endo- and myocardial circumferential strain might be related to the presence and extent of fibrosis, whilst future studies are required to further evaluate the potential added value of measuring strain in specific layers.

Interestingly, no significant association between LV rotational parameters and myocardial fibrosis, nor a correlation with the extent of fibrosis was observed. Previous research by *Taylor* et al. found an association between rotational parameters and fibrosis albeit in adult patients with non-ischemic cardiomyopathy, reduced LVEF (±27%), and severely decreased GCS (± −10%) [33]. In patients with DMD, differences in LV twist using CMR tagging were observed compared to healthy controls, but the relation with fibrosis was not investigated [34]. Although one needs to consider the variation when assessing LV rotation using CMR-FT [35], we found no association with presence or extent of cardiac fibrosis. A possible explanation could be that rotation is only affected when circumferential contraction, i.e., strain, is sufficiently affected.

In our cohort, myocardial fibrosis was most frequently located in inferolateral and anterolateral segments, confirming previous observations in DMD [3,36]. No clear pattern between segmental strain and fibrosis location was observed. A first potential explanation may relate to the variability reported when assessing segmental strain using CMR-FT. Segmental strain seems associated with estimation errors, possibly hampering accurate measurement [35,37]. A second explanation relates to pathophysiology. The loss of membrane stability permits, amongst others, influx of calcium, altered mitochondrial energetics, and myocyte loss, which may be a diffuse rather than a focal process in DMD [38].

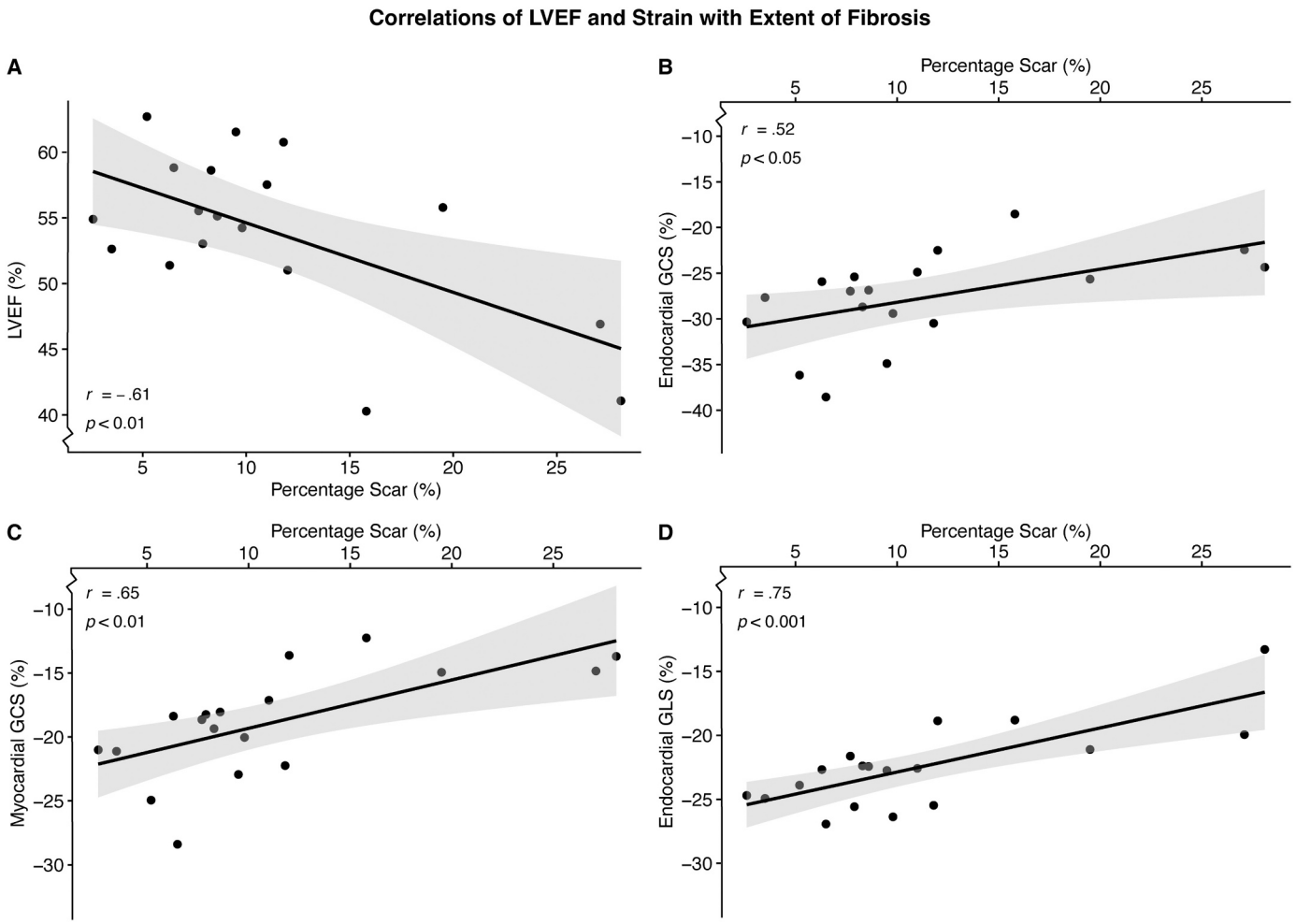

Fig. 1. Correlation of LV scar % with (A) left ventricular ejection fraction (LVEF), (B) endocardial global circumferential strain (GCS), (C) myocardial global circumferential strain (GCS), and (D) endocardial global longitudinal strain (GLS) in the patients with myocardial fibrosis (n = 18). The dotted line represents the line of best fit and the gray area represents the 95% confidence interval. r = Pearson correlation coefficient; p = *p*-value.

Accordingly, myocardial function and structure might be diffusely altered, whilst these changes might remain undetected by LGE [39,40]. This could account for the observed heterogeneity in segmental strain values and fibrosis distribution, as also observed in patients with dilated cardiomyopathy [41]. Taken together, we found no relation between segmental strain and fibrosis in DMD patients, which may, at least in part, be related to limitations in spatial resolution to assess segmental strain and fibrosis. We recommend future studies also investigating (post contrast) T1-mapping, which could aid in assessment alterations in myocardial structure [42].

4.1. Strengths & Limitations

The small cohort size possibly affects the ability to detect parameters associated with fibrosis and limits correction for possible confounders. However, including only exams with high image quality increased robustness and allowed us to provide meaningful insight. Secondly, although validated, CMR-FT shows more variation than CMR tagging and uses endocardial and epicardial border tracking instead of physical intra-tissue markers [43]. However CMR-FT has been shown to be reproducible [35], and is clinically widely applicable since no additional image acquisition is required.

4.2. Future perspective

Our study revealed a possible association between LV strain parameters and the presence and extent of fibrosis in DMD. Although future, larger-sized studies are warranted, the potential clinical impact is obvious if it could replace the administration of contrast agents to evaluate presence or risk of fibrosis. Especially since strain-derived indices, such as surface area strain and mechanical dyssynchrony, could be promising markers [44,45]. Moreover, CMR-FT might provide markers to monitor (changes in) the extent of cardiac fibrosis. In this respect, it is important to highlight that strain showed stronger relation to the presence and magnitude of fibrosis than LVEF. However, to improve understanding of the interplay between functional parameters and disease progression, repeated measures are required. The importance thereof seems illustrated by the variability in our cohort and as presented by others between patients of similar age [46]. This further warrants studies to better understand the potential of strain parameters to evaluate individual patients and to potentially guide and personalize treatment.

In conclusion, this study found that lower endocardial global circumferential (GCS) and longitudinal strain (GLS) was associated with presence of LV myocardial fibrosis in pediatric patients with Duchenne muscular dystrophy, which remained significant for GCS when adjusting for age. Additionally, both GCS and GLS correlated with the extent of fibrosis. Therefore, strain parameters may be valuable markers to monitor presence and/or progression of cardiac fibrosis in DMD.

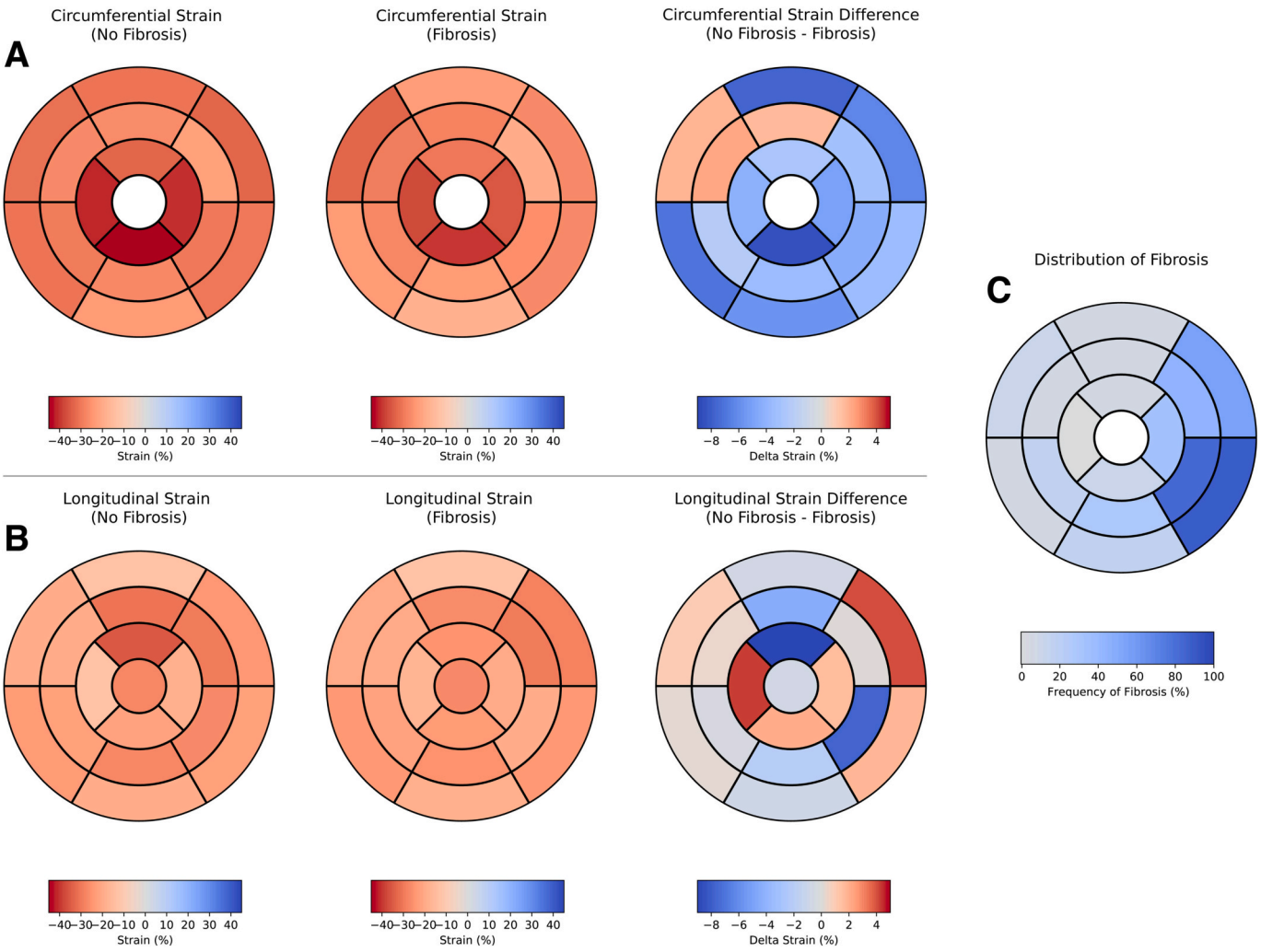

Fig. 2. Strain patterns comparing segmental strain values between the groups without and with fibrosis. (A) Endocardial circumferential segmental strain. Circumferential Strain Difference represents segmental strain difference between groups (No Fibrosis – Fibrosis). (B) Endocardial longitudinal segmental strain. Longitudinal Strain Difference represents segmental strain difference between groups (No Fibrosis – Fibrosis). A lower segmental strain for the fibrosis group results in a negative (blue) value in the circumferential strain difference bullseye. (C) Distribution of fibrosis within the fibrosis group. For circumferential strain and fibrosis occurrence, the apex was not assessed. (For interpretation of the references to colour in this figure legend, the reader is referred to the web version of this article.)

Author contributions

TK, WE, JH, DT, and FU were involved in the conception and design. All authors were involved in analysis and interpretation of the results. TK, WE, and DT prepared the draft of the manuscript. All authors reviewed the results, revised it critically for important intellectual content, and approved the final version of the manuscript and agree to be accountable for all aspects of the work.

Funding

TK received a personal grant from Radboudumc for his work.

Declaration of Competing Interest

None to declare.

Data availability

The analyzed dataset, underlying this manuscript, will be shared upon reasonable request to the corresponding author.

Acknowledgements

We thank Isaïa Seguinot for her help with exploring and analyzing the data during her internship. TK received a personal grant from Radboudumc for his research.

References

[1] D.J. Birnkrant, K. Bushby, C.M. Bann, S.D. Apkon, A. Blackwell, D. Brumbaugh, et al., Diagnosis and management of Duchenne muscular dystrophy, part 1: diagnosis, and neuromuscular, rehabilitation, endocrine, and gastrointestinal and nutritional management, Lancet Neurol. 17 (3) (2018) 251–267.
[2] S. Ryder, R.M. Leadley, N. Armstrong, M. Westwood, S. de Kock, T. Butt, et al., The burden, epidemiology, costs and treatment for Duchenne muscular dystrophy: an evidence review, Orphanet. J. Rare Dis. 12 (1) (2017) 79.
[3] F. Kamdar, D.J. Garry, Dystrophin-deficient cardiomyopathy, J. Am. Coll. Cardiol. 67 (21) (2016) 2533–2546.
[4] A.E. Emery, The muscular dystrophies, Lancet. 359 (9307) (2002) 687–695.
[5] H. Van Ruiten, K. Bushby, M. Guglieri, State-Of-The-Art Advances in Duchenne Muscular Dystrophy, EMJ 2 (1) (2017) 90–99.
[6] M. Eagle, S.V. Baudouin, C. Chandler, D.R. Giddings, R. Bullock, K. Bushby, Survival in Duchenne muscular dystrophy: improvements in life expectancy since 1967 and the impact of home nocturnal ventilation, Neuromuscul. Disord. 12 (10) (2002) 926–929.
[7] G. Nigro, L.I. Comi, L. Politano, R.J. Bain, The incidence and evolution of cardiomyopathy in Duchenne muscular dystrophy, Int. J. Cardiol. 26 (3) (1990) 271–277.

[8] P. Magrath, N. Maforo, P. Renella, S.F. Nelson, N. Halnon, D.B. Ennis, Cardiac MRI biomarkers for Duchenne muscular dystrophy, Biomark. Med 12 (11) (2018) 1271–1289.
[9] D.J. Birnkrant, K. Bushby, C.M. Bann, B.A. Alman, S.D. Apkon, A. Blackwell, et al., Diagnosis and management of Duchenne muscular dystrophy, part 2: respiratory, cardiac, bone health, and orthopaedic management, Lancet Neurol. 17 (4) (2018) 347–361.
[10] E. Potter, T.H. Marwick, Assessment of left ventricular function by echocardiography: the case for routinely adding global longitudinal strain to ejection fraction, JACC Cardiovasc. Imaging 11 (2, Part 1) (2018) 260–274.
[11] G. Song, J. Zhang, X. Wang, X. Zhang, F. Sun, X. Yu, Usefulness of speckle-tracking echocardiography for early detection in children with Duchenne muscular dystrophy: a meta-analysis and trial sequential analysis, Cardiovasc. Ultrasound 18 (1) (2020) 26.
[12] K.N. Hor, J. Wansapura, L.W. Markham, W. Mazur, L.H. Cripe, R. Fleck, et al., Circumferential strain analysis identifies strata of cardiomyopathy in Duchenne muscular dystrophy: a cardiac magnetic resonance tagging study, J. Am. Coll. Cardiol. 53 (14) (2009) 1204–1210.
[13] L. Wu, T. Germans, A. Güçlü, M.W. Heymans, C.P. Allaart, A.C. van Rossum, Feature tracking compared with tissue tagging measurements of segmental strain by cardiovascular magnetic resonance, J. Cardiovasc. Magn. Reson. 16 (1) (2014) 10.
[14] P. Amedro, M. Vincenti, G. De La Villeon, K. Lavastre, C. Barrea, S. Guillaumont, et al., Speckle tracking echocardiography in children with Duchenne muscular dystrophy: a multicenter controlled cross-sectional study, Arch. Cardiovasc. Diseas. Suppl. 11 (1) (2019) 58.
[15] S. Ünlü, O. Mirea, E.D. Pagourelias, J. Duchenne, S. Bézy, J. Bogaert, et al., Layer-specific segmental longitudinal strain measurements: capability of detecting myocardial scar and differences in feasibility, accuracy, and reproducibility, among four vendors a report from the EACVI-ASE strain standardization task force, J. Am. Soc. Echocardiogr. 32 (5) (2019), 624–632.e11.
[16] P.P. Sengupta, A.J. Tajik, K. Chandrasekaran, B.K. Khandheria, Twist mechanics of the left ventricle: principles and application, JACC Cardiovasc. Imaging 1 (3) (2008) 366–376.
[17] T. Karaahmet, E. Gürel, K. Tigen, A. Güler, C. Dündar, H. Fotbolcu, et al., The effect of myocardial fibrosis on left ventricular torsion and twist in patients with non-ischemic dilated cardiomyopathy, Cardiol. J. 20 (3) (2013) 276–286.
[18] A.M.S. Omar, S. Vallabhajosyula, P.P. Sengupta, Left ventricular twist and torsion. Circulation, Cardiovascular Imaging. 8 (6) (2015), e003029.
[19] A. Dubrovsky, E. Guevara, P. Locatelli, L. Mesa, A. Jauregui, P1.15 left ventricular torsion analysis in Duchenne muscular dystrophy, Neuromuscul. Disord. 21 (9) (2011) 646.
[20] E. Heiberg, J. Sjögren, M. Ugander, M. Carlsson, H. Engblom, H. Arheden, Design and validation of Segment–freely available software for cardiovascular image analysis, BMC Med. Imaging 10 (2010) 1.
[21] M.D. Cerqueira, N.J. Weissman, V. Dilsizian, A.K. Jacobs, S. Kaul, W.K. Laskey, et al., Standardized myocardial segmentation and nomenclature for tomographic imaging of the heart. A statement for healthcare professionals from the cardiac imaging Committee of the Council on clinical cardiology of the American Heart Association, Circulation. 105 (4) (2002) 539–542.
[22] J.U. Voigt, G. Pedrizzetti, P. Lysyansky, T.H. Marwick, H. Houle, R. Baumann, et al., Definitions for a common standard for 2D speckle tracking echocardiography: consensus document of the EACVI/ASE/industry task force to standardize deformation imaging, J. Am. Soc. Echocardiogr. 28 (2) (2015) 183–193.
[23] S. Nakatani, Left ventricular rotation and twist: why should we learn? J. Cardiovasc. Ultrasound. 19 (1) (2011) 1–6.
[24] R Development Core Team, R: A Language and Environment for Statistical Computing, R Foundation for Statistical Computing, Vienna, Austria, 2021.
[25] F.J. Raucci, M. Xu, K. George-Durrett, K. Crum, J.C. Slaughter, D.A. Parra, et al., Non-contrast cardiovascular magnetic resonance detection of myocardial fibrosis in Duchenne muscular dystrophy, J. Cardiovasc. Magn. Reson. 23 (1) (2021) 48.
[26] G. Morton, A. Schuster, R. Jogiya, S. Kutty, P. Beerbaum, E. Nagel, Inter-study reproducibility of cardiovascular magnetic resonance myocardial feature tracking, J. Cardiovasc. Magn. Reson. 14 (1) (2012) 43.
[27] O.A. Smiseth, H. Torp, A. Opdahl, K.H. Haugaa, S. Urheim, Myocardial strain imaging: how useful is it in clinical decision making? Eur. Heart J. 37 (15) (2016) 1196–1207.
[28] M.D. Puchalski, R.V. Williams, B. Askovich, C.T. Sower, K.H. Hor, J.T. Su, et al., Late gadolinium enhancement: precursor to cardiomyopathy in Duchenne muscular dystrophy? Int. J. Card. Imaging 25 (1) (2009) 57–63.
[29] A. Azzu, A.S. Antonopoulos, S. Krupickova, Z. Mohiaddin, B. Almogheer, C. Vlachopoulos, et al., Myocardial strain analysis by cardiac magnetic resonance 3D feature-tracking identifies subclinical abnormalities in patients with neuromuscular disease and no overt cardiac involvement, Eur. Heart J. Cardiovasc. Imaging 24 (4) (2023) 503–511.
[30] J.H. Soslow, M. Xu, J.C. Slaughter, K. Crum, J.A. Kaslow, K. George-Durrett, et al., Cardiovascular measures of all-cause mortality in Duchenne muscular dystrophy, Circ. Heart Fail. (2023), 0(0):e010040.
[31] R. Tanacli, D. Hashemi, T. Lapinskas, F. Edelmann, R. Gebker, G. Pedrizzetti, et al., Range variability in CMR feature tracking multilayer strain across different stages of heart failure, Sci. Rep. 9 (1) (2019) 16478.
[32] S. Ünlü, O. Mirea, E.D. Pagourelias, J. Duchenne, S. Bézy, J. Bogaert, et al., Layer-specific segmental longitudinal strain measurements: capability of detecting myocardial scar and differences in feasibility, accuracy, and reproducibility, among four vendors a report from the EACVI-ASE strain standardization task force, J. Am. Soc. Echocardiogr. 32 (5) (2019), 624–32.e11.
[33] R. Taylor, F. Umar, E. Lin, A. Ahmed, W. Moody, W. Mazur, et al., Mechanical effects of left ventricular midwall fibrosis in non-ischemic cardiomyopathy, J. Cardiovasc. Magn. Reson. 18 (2016) 1.
[34] M.L. Reyhan, Z. Wang, H.J. Kim, N.J. Halnon, J.P. Finn, D.B. Ennis, Effect of free-breathing on left ventricular rotational mechanics in healthy subjects and patients with duchenne muscular dystrophy, Magn. Reson. Med. 77 (2) (2017) 864–869.
[35] G. Pedrizzetti, P. Claus, P.J. Kilner, E. Nagel, Principles of cardiovascular magnetic resonance feature tracking and echocardiographic speckle tracking for informed clinical use, J. Cardiovasc. Magn. Reson. 18 (1) (2016) 51.
[36] K.C. Bilchick, M. Salerno, D. Plitt, Y. Dori, Crawford TO, D. Drachman, et al., Prevalence and distribution of regional scar in dysfunctional myocardial segments in Duchenne muscular dystrophy, J. Cardiovasc. Magn. Reson. 13 (1) (2011) 20.
[37] M. Dobrovie, M. Barreiro-Pérez, D. Curione, R. Symons, P. Claus, J.-U. Voigt, et al., Inter-vendor reproducibility and accuracy of segmental left ventricular strain measurements using CMR feature tracking, Eur. Radiol. 29 (12) (2019) 6846–6857.
[38] T.A. Meyers, D. Townsend, Cardiac pathophysiology and the future of cardiac therapies in Duchenne muscular dystrophy, Int. J. Mol. Sci. 20 (17) (2019).
[39] P. Haaf, P. Garg, D.R. Messroghli, D.A. Broadbent, J.P. Greenwood, S. Plein, Cardiac T1 mapping and extracellular volume (ECV) in clinical practice: a comprehensive review, J. Cardiovasc. Magn. Reson. 18 (1) (2016) 89.
[40] J.H. Soslow, B.M. Damon, B.R. Saville, Z. Lu, W.B. Burnette, M.A. Lawson, et al., Evaluation of post-contrast myocardial t1 in duchenne muscular dystrophy using cardiac magnetic resonance imaging, Pediatr. Cardiol. 36 (1) (2015) 49–56.
[41] C. Chevalier, K. Kremer, E. Cavus, J. Schneider, C. Jahnke, G. Schön, et al., CMR feature tracking in patients with dilated cardiomyopathy: patterns of myocardial strain and focal fibrosis, Open Heart. 9 (2) (2022), e002013.
[42] E. Riesenkampff, D.R. Messroghli, A.N. Redington, L. Grosse-Wortmann, Myocardial T1 mapping in pediatric and congenital heart disease, Circ. Cardiovasc. Imag. 8 (2) (2015), e002504.
[43] M.S. Amzulescu, M. De Craene, H. Langet, A. Pasquet, D. Vancraeynest, A. C. Pouleur, et al., Myocardial strain imaging: review of general principles, validation, and sources of discrepancies, Eur. Heart J. Cardiovasc. Imaging 20 (6) (2019) 605–619.
[44] C.C. Earl, V.I. Pyle, S.Q. Clark, K. Annamalai, P.A. Torres, A. Quintero, et al., Localized strain characterization of cardiomyopathy in Duchenne muscular dystrophy using novel 4D kinematic analysis of cine cardiovascular magnetic resonance, J. Cardiovasc. Magn. Reson. 25 (1) (2023) 14.
[45] K.N. Hor, J.P. Wansapura, H.R. Al-Khalidi, W.M. Gottliebson, M.D. Taylor, R. J. Czosek, et al., Presence of mechanical dyssynchrony in duchenne muscular dystrophy, J. Cardiovasc. Magn. Reson. 13 (1) (2011) 12.
[46] J. Kwiatkowska, J. Meyer-Szary, M. Bazgier, J. Fijałkowska, J. Wierzba, A. Glińska, et al., Left ventricular volumes and function affected by myocardial fibrosis in patients with Duchenne and Becker muscular dystrophies: a preliminary magnetic resonance study, Kardiol. Pol. 78 (4) (2020) 331–334.